

Accepted Manuscript

Research paper

In situ oxidation triggered heteroleptically deprotonated Cobalt(III) and homoleptic Nickel(II) complexes of diacetyl monoxime derived tri-nitrogen chelators; Synthesis, molecular structures and Biological assay.

Vinayak Kamat, Avinash Kotian, Anupama Nevarekar, Krishna Naik, Dhoolesh Kokare, Vidyanand K. Revankar

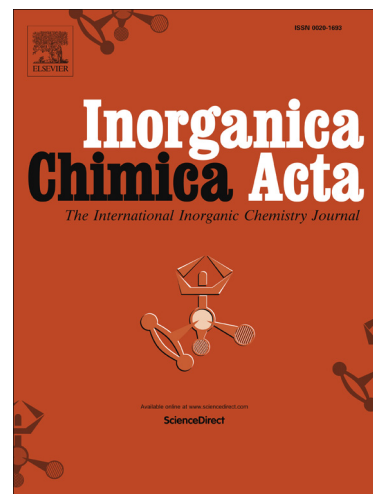
PII: S0020-1693(17)30525-X
DOI: <http://dx.doi.org/10.1016/j.ica.2017.07.036>
Reference: ICA 17759

To appear in: *Inorganica Chimica Acta*

Received Date: 10 April 2017
Revised Date: 13 July 2017
Accepted Date: 14 July 2017

Please cite this article as: V. Kamat, A. Kotian, A. Nevarekar, K. Naik, D. Kokare, V.K. Revankar, *In situ* oxidation triggered heteroleptically deprotonated Cobalt(III) and homoleptic Nickel(II) complexes of diacetyl monoxime derived tri-nitrogen chelators; Synthesis, molecular structures and Biological assay., *Inorganica Chimica Acta* (2017), doi: <http://dx.doi.org/10.1016/j.ica.2017.07.036>

This is a PDF file of an unedited manuscript that has been accepted for publication. As a service to our customers we are providing this early version of the manuscript. The manuscript will undergo copyediting, typesetting, and review of the resulting proof before it is published in its final form. Please note that during the production process errors may be discovered which could affect the content, and all legal disclaimers that apply to the journal pertain.



***In situ* oxidation triggered heteroleptically deprotonated Cobalt(III) and homoleptic Nickel(II) complexes of diacetyl monoxime derived tri-nitrogen chelators; Synthesis, molecular structures and Biological assay.**

Vinayak Kamat^a, Avinash Kotian^a, Anupama Nevarekar^a, Krishna Naik^a, Dhoolesh Kokare^a and Vidyanand K. Revankar^{a*}

^aDepartment of Chemistry, Karnatak University, Dharwad-580003, India.

* Corresponding author

Abstract: Two tri-nitrogen chelating unsymmetrical Schiff base ligands, 3-(hydroxyimino)-2-butanone-2-(1*H*-benzothiazol-2-yl)hydrazone and 3-(hydroxyimino)-2-butanone-2-(1*H*-benzimidazol-2-yl)hydrazone are synthesized by the condensation reaction of diacetyl monoxime with 2-hydrazino-benzothiazole/benzimidazole. Ligands have shown ML₂ type octahedral coordination towards Ni(II) and *in situ* generated Co(III) ions. Ligands and complexes are characterized by various spectro-analytical techniques. Both the ligands have shown a similar mode of ligation, but a different mode of deprotonation towards the cobalt and nickel ions. Ligands are left neutral in the case of nickel complexes while anionic in the case of cobalt complexes. Further, *in situ* oxidation of Co(II) to Co(III) has triggered a different mode of deprotonation between the two ligands of the same cobalt complex. Out of the four complexes synthesized, three complexes are characterized by single crystal X-ray diffraction technique, to evidence the structural facts. A comparative account of bond lengths of two complexes of the bezothiazole based ligand is presented. Structures of all the four complexes have been checked preliminarily for their NCI-60 Human Cancer Cell Line anticancer screening. Further, one among the four, the nickel complex of benzothiazole core is used for one dose growth inhibition screening against 60 different human cancer cell lines. The tested complex has shown highest growth inhibition over a Non-Small Cell Lung Cancer cell line EKVX. In addition, compounds are screened for their antibacterial and antifungal potencies against few microorganisms. The complexes have shown promising antimicrobial potencies.

Keywords: Diacetyl monoxime, Benzothiazole Schiff base, 2-hydrazinobenzimidazole, Heteroleptic deprotonation, Co(III) complexes.

Highlights :

- Two new tridentate ligands 3-(hydroxyimino)-2-butanone-2-(1*H*-benzothiazol-2-yl)hydrazone and 3-(hydroxyimino)-2-butanone-2-(1*H*-benzimidazol-2-yl)hydrazone are synthesized and characterized.
- Ni(II) and *in situ* generated Co(III) complexes of the ligands are synthesized and characterized by the single crystal X-ray diffraction method.
- Ligands are left neutral in the case of nickel complexes while anionic in the case of cobalt complexes.
- One dose growth inhibition screening against 60 different human cancer cell lines is carried out for Nickel complex of benzothiazole core.
- Ligands and complexes are tested for their antibacterial and antifungal potencies.

1. Introduction

Transition metal complexes of hydrazone based Schiff base ligands have attracted the coordination chemists for a long time. Substituted organic heterocycles with donor atoms in tuned positions have readily found their use in designing such ligand systems [1-4]. Benzothiazoles and benzimidazoles are the class of organic heterocycles, which have imparted biological applications to their transition metal complexes, antitumor and antimicrobial assessments being predominant. [5-8].

Due to their structure, stability and reactivity, oximes have kindled the interest in designing ligand systems for transition metal ions [9, 10]. The oxime functionality is amphiprotic with a mildly acidic hydroxyl group and slightly basic nitrogen atom [11]. Hence it is widely recognized to produce different modes of coordination [12]. The structural diversity of oxime ligands varies from mononuclear to higher nuclearity via oximate bridges [13]. But mononuclear octahedral complexes are preferred if the ligand provides a stable tridentate mode of coordination [11, 14].

ML₂ type cobalt complexes of tridentate hydrazones, often show *in situ* oxidation of Co(II) to Co(III) [15]. In such complexes with uninegative tridentate Schiff bases, electric neutrality is maintained by the presence of a counter anion [16]. In contrast,

Co(III) complexes with dinegative tridentate ligands have received less attention. In addition, transition metal complexes, particularly Co(III) complexes derived from unsymmetrical and symmetrical Schiff bases have drawn considerable attention in the past for their important biological applications [17]. These facts have motivated the present work, wherein synthesis, structural characterization and biological evaluation of four novel transition metal complexes are undertaken.

2. Experimental

2.1. Materials and physical measurements

Diacetyl monoxime obtained from Thomas-Baker and other reagents including 2-mercaptobenzimidazole/benzothiazole obtained from SD-Fine Chemicals were used as supplied. Solvents were purified and dried according to the standard procedures. The metal salts used were in their hydrated form, i.e., $\text{CoCl}_2 \cdot 6\text{H}_2\text{O}$, $\text{NiCl}_2 \cdot 6\text{H}_2\text{O}$. Reaction progress was maintained through silica gel thin layer chromatographic technique.

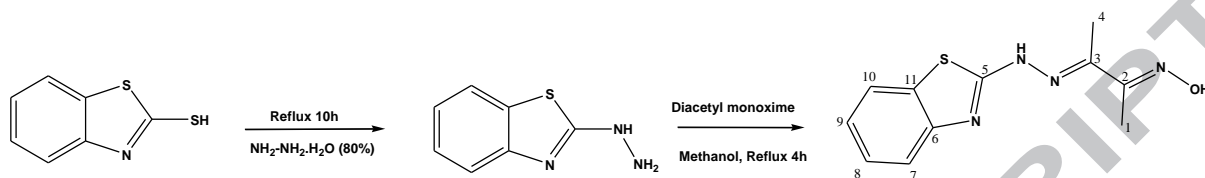
The CHN analysis was performed on a Thermo quest elemental analyzer. Molecular weights and formulae were calculated without solvent molecules unless explicitly stated. The ^1H NMR spectra were recorded on AGILENT VNMRS-400/JEOL ECX-500 spectrometer, in a $\text{DMSO}-d_6$ solvent. Infrared spectra were recorded in KBr discs in the region $4000\text{--}400\text{ cm}^{-1}$ on a Nicolet-6700 FT-IR spectrometer. The solution state UV-Vis spectra of all the compounds in methanol were recorded on a JASCO V-670 UV-Vis spectrophotometer. The EI mass spectrum of the ligand was obtained with a Shimadzu GCMS-QP2010S spectrometer. The ESI mass spectral data for all the complexes were obtained using a Waters UPLCTQD mass spectrometer. Magnetic susceptibility measurements were carried out on polycrystalline samples, using a Faraday balance at room temperature with $\text{Hg}[\text{Co}(\text{SCN})_4]$ as reference.

2.2. Synthesis of Ligands

2.2.1. 3-(hydroxyimino)-2-butanone-2-(1H-benzothiazol-2-yl)hydrazone (L^1H_2)

The schematic representation of the synthesis of L^1H_2 is given in Scheme 1. First, 2-hydrazinobenzothiazole was obtained from 2-mercaptobenzothiazole by the reported method [18]. In the next step, 2-hydrazinobenzothiazole (1.65 g, 0.01 mol) was refluxed

with diacetyl monoxime (1.01g, 0.01 mol) in 20 mL of methanol for 1 h. On cooling, the separated white slimy product was filtered and washed with cold methanol. The solid product was dried in vacuo for 4 h.



Scheme 1 Synthesis of L^1H_2 .

Yield: 83%. M.P.: 280°C. Color: white; Anal. Calc. for $C_{11}H_{12}N_4OS$ (%): C, 53.21; H, 4.87; N, 22.56. Found for L^1H_2 (%): C, 53.53; H, 5.01; N, 22.32. 1H NMR (400 MHz, DMSO- d_6): δ (ppm) 11.66 (s, 1H, OH), 11.46 (s, 1H, NH), 7.70-7.05 (m, 4H, $C_7 - C_{10}H$), 2.11 (s, 3H, C_1H), 2.01 (s, 3H, C_4H). EI-MS (m/z): 248 (M^+). IR (KBr, v , cm^{-1}): 3442, 1612, 1571, 1545, 750. λ_{max} (nm): 231 ($\pi \rightarrow \pi^*$), 313 ($n \rightarrow \pi^*$).

2.2.2. 3-(hydroxyimino)-2-butanone-2-(1H-benzimidazol-2-yl)hydrazone (L^2H_2)

The synthesis of L^1H_2 was carried out according to the previously developed strategy [19].

Yield: 55%. M.P.: 240°C. Color: buff. Anal. Calc. for $C_{13}H_{17}N_5O_3$ (%): C, 53.60; H, 5.88; N, 24.04. Found for L^2H_2 (%): C, 53.91; H, 5.43; N, 23.72. 1H NMR (400 MHz, DMSO- d_6): δ (ppm) 11.36 (b, 2H, OH and NH), 7.23 - 7.21 (m, 2H, C_7H and $C_{10}H$), 6.96 - 6.94 (m, 2H, C_8H and C_9H), 3.15 (s, 2H, ring NH), 2.12 (s, 3H, C_1H), 2.09 (s, 3H, C_4H), 1.88 (s, 3H, $C_{13}H$). EI-MS (m/z): 231 (M^+). IR (KBr, v , cm^{-1}): 3516, 3168, 1673, 1016, 748. λ_{max} (nm): 218 ($\pi \rightarrow \pi^*$), 305 ($n \rightarrow \pi^*$).

2.3. Syntheses of metal complexes

The complexes were obtained by refluxing the respective hexa hydrated metal chlorides (0.119 g, 0.500 mmol) with the methanolic solution of ligands (L^1H_2 0.248 g or L^2H_2 0.231 g, 1.00 mmol) for 4 h. The crystalline product was obtained by evaporating the solvent under reduced pressure. Single crystals were obtained by evaporating the methanolic solution of respective complexes.

2.3.1. [Co(L¹H)(L)]

Yield: 84%. Color: red. Anal. Calc. for C₂₂H₂₁N₈O₂S₂Co (%): C, 47.82; H, 3.83; N, 20.28. Found for [Co(L¹H)(L)] (%): C, 47.53; H, 3.48; N, 19.92. ¹H NMR (500 MHz, DMSO-d₆): δ (ppm) 10.65 (s, 1H, OH), 7.43-6.82 (m, 8H, C₇ - C₁₀H), 2.64 (s, 6H, C₁H), IR (KBr, ν, cm⁻¹): 3380, 1586, 1437, 1016, 747, 489. λ_{max} (nm): 219 (π→π*), 287(n→π*), 487(LMCT). ESI-MS (positive mode m/z): 553.

2.3.2. [Co(L²H)(L)]

Yield: 69%. Color: red. Anal. Calc. for C₂₂H₂₃N₁₀O₂Co (%): C, 50.97; H, 4.47; N, 27.02. Found for [Co(L²H)(L)] (%): C, 51.33; H, 4.15; N, 27.42. ¹H NMR (500 MHz, DMSO-d₆): δ (ppm) 12.25 (s, 2H, ring NH), 11.80 (s, 1H, OH), 6.96 - 6.56 (m, 8H, C₇H - C₁₀H), 2.68 (s, 6H, C₁H), 2.19 (s, 6H, C₄H). IR (KBr, ν, cm⁻¹): 3373, 1657, 1627, 1591, 1456, 751. λ_{max} (nm): 213 (π→π*), 296(n→π*), 476(LMCT). ESI-MS (positive mode m/z): 519.

2.3.3. [Ni(L¹H₂)₂]Cl₂

Yield: 88%. Color: yellow. Anal. Calc. for C₂₂H₂₄N₈O₂S₂NiCl₂ (%): C, 42.20; H, 3.86; N, 17.89. Found for [Ni(L¹H₂)₂]Cl₂ (%): C, 42.54; H, 3.56; N, 18.22. IR (KBr, ν, cm⁻¹): 3394, 1578, 1519, 1073, 752, 464. λ_{max} (nm): 220 (π→π*), 313(n→π*), 828(d-d transtion). ESI-MS (positive mode m/z): 553, 249.

2.3.4. [Ni(L²H₂)₂]Cl₂

Yield: 54%. Color: yellow. Anal. Calc. for C₂₂H₂₆N₁₀O₂NiCl₂ (%): C, 44.63; H, 4.43; N, 23.66. Found for [Ni(L²H₂)₂]Cl₂ (%): C, 44.44; H, 4.18; N, 23.28. IR (KBr, ν, cm⁻¹): 3383, 1650, 1578, 747. λ_{max} (nm): 211 (π→π*), 300(n→π*), 818(d-d transtion). ESI-MS (positive mode m/z): 519, 232.

2.4. Crystallographic data collection and refinement

The single crystal X-ray diffraction data were obtained at 296 K on a Bruker SMART APEX2 CCD area detector diffractometer using a graphite monochromated Mo-Kα (λ = 0.71073 Å) radiation source. Bruker SAINT Software package [20] was used to integrate the frames using a narrow-frame algorithm. The structure was solved on Olex2 [21] with ShelXT [22] structure solution program using Intrinsic Phasing and refined

with the XL [23] refinement package using Least Squares minimization. All non-hydrogen atoms were refined anisotropically. A summary of the crystallographic data and structure refinement for $[\text{Co}(\text{L}^1\text{H})(\text{L}^1)]$ and $[\text{Ni}(\text{L}^2\text{H}_2)_2]\text{Cl}_2$ are tabulated in table 1, while the data for $[\text{Ni}(\text{L}^2\text{H}_2)_2]\text{Cl}_2$ is provided in the supplementary information (SI) along with other geometric tables (SI-T1 to SI-T5). The mercury-3.8 package was used to generate molecular graphics [24].

Table 1. Crystallographic data and structure refinement

	$[\text{Co}(\text{L}^1\text{H})(\text{L}^1)]$	$[\text{Ni}(\text{L}^1\text{H}_2)_2]\text{Cl}_2$
Crystal data		
Chemical formula	$\text{C}_{22}\text{H}_{21}\text{CoN}_8\text{O}_2\text{S}_2$	$\text{C}_{22}\text{H}_{24}\text{N}_8\text{NiO}_2\text{S}_2 \cdot 2(\text{Cl}) \cdot 2(\text{H}_2\text{O}) \cdot \text{O}$
M_r	552.52	678.25
Crystal system, space group	Monoclinic, $P2_1/c$	Triclinic, $P-1$
Temperature (K)	296	296
a, b, c (Å)	10.2921 (2), 13.8972 (3), 17.0674 (3)	10.6157 (2), 11.3691 (2), 13.4250 (2)
α, β, γ (°)	$\beta = 93.979$ (1)	100.160 (1), 99.940 (1), 101.713(1)
V (Å ³)	2435.29 (8)	1524.71 (5)
Z	4	2
Radiation type	Mo $K\alpha$	Mo $K\alpha$
μ (mm ⁻¹)	0.91	0.99
Crystal size (mm)	0.25 × 0.15 × 0.1	0.3 × 0.15 × 0.1
Data collection		
Diffractometer	Bruker APEX-II CCD	Bruker APEX-II CCD
No. of measured, independent and observed [$I > 2\sigma(I)$] reflections	39089, 10467, 7875	19485, 5352, 4456
R_{int}	0.026	0.029

$(\sin \theta/\lambda)_{\max}$ (\AA^{-1})	0.802	0.595
Refinement		
$R[F^2 > 2\sigma(F^2)]$, $wR(F^2)$, S	0.037, 0.107, 1.03	0.039, 0.112, 1.05
No. of reflections	10467	5352
No. of parameters	356	419
H-atom treatment	Mixed	Mixed
$\Delta\rho_{\max}$, $\Delta\rho_{\min}$ ($e \text{\AA}^{-3}$)	0.48, -0.41	0.77, -0.67

2.5. NCI-60 Human Cancer Cell Line Screening Methodology

The compound $[\text{Ni}(\text{L}^1\text{H}_2)_2]\text{Cl}_2$ was tested against a panel of 60 human cancer cell lines at the National Cancer Institute, Rockville, MD[25]. The cytotoxicity studies were conducted using a 48 h exposure protocol using the sulforhodamine B assay [26, 27].

The One-dose data was reported as the percent growth inhibition (GI %) of treated cells. The number reported is growth relative to the no-drug control and relative to the time zero number of cells. This has allowed detection of both growth inhibition (values between 0 and 100) and lethality (values less than 0).

2.6. Growth inhibitory activity of microbial strains[28]

The MIC values of ligands and complexes for the growth inhibition of six different pathogenic microbial genomes *S. epidermidis*, *E. faecalis*, *K. pneumoniae*, *E. coli*, *A. fumigatus* and *C. albicans* were determined in HIMEDIA M210 Brain heart infusion (BHI) broth. This is used for the propagation of pathogenic cocci and other fastidious organisms associated with allied pathological investigations. BHI broth had the following composition.

Ingredients in g/L. Calf brain, infusion from, 200.00; Beef heart infusion from, 250.00; Proteose peptone, 10.00; Dextrose, 2.00; Sodium chloride, 5.00; Disodium phosphate, 2.50. And the final pH (at 25°C) was 7.4+/-0.2.

Nine dilutions of each sample were done with BHI for MIC determination. In the initial tube, 20 μL of the drug was added to the 380 μL of BHI broth. Then, 200 μL of BHI broth was added into the next 9 tubes separately for dilution. From the initial tube, 200 μL was transferred to the first tube containing 200 μL of BHI broth. This was considered as 10^{-1} dilution. From 10^{-1} diluted tube, 200 μL was transferred to the second tube to make 10^{-2} dilution. The serial dilution was repeated up to 10^{-9} dilution for each drug. From the maintained stock cultures of required organisms, 5 μL was taken and added into 2 mL of BHI broth. In each serially diluted tube, 200 μL of above culture suspension was added. The tubes were incubated for 24 hours and observed for turbidity.

3. Results and Discussion

The primary aim of the work was to synthesize Co(II) and Ni(II) complexes of newly designed, structurally interesting ligand systems. Accordingly, the ligands L^1H_2 and L^2H_2 were synthesized by condensing diacetyl monoxime with 2-hydrazinobenzothiazole/benzimidazole. These ligands are of structural interest, due to their different possible modes of deprotonation and coordination. But in the present case, a stable ML_2 type of tri-nitrogen chelation is observed in all the four complexes. Ionizable protons in the ligands being moderately acidic, deprotonation has depended itself on the metal salt tuned pH. Hence the ligands behaved neutrally with nickel centers, while anionic with the cobalt centers. Further, *in situ* oxidation of Co(II) to Co(III) during complexation has made the ligands of cobalt complexes heteroleptically deprotonated.

All the complexes are soluble in methanol, ethanol, acetone and DMSO. The analytical and spectroscopic data for ligands and complexes are presented in the experimental section. The analytical data and spectral characterization results of all the complexes are consistent with the proposed structures. Cobalt complexes are diamagnetic, as expected for low spin octahedral Co(III) complexes. This observation is further supported by sharp signals in the diamagnetic region of ^1H NMR of these complexes. The observed magnetic moments of 3.10 and 3.18 BM for $[\text{Ni}(\text{L}^1\text{H}_2)_2]\text{Cl}_2$ and $[\text{Ni}(\text{L}^2\text{H}_2)_2]\text{Cl}_2$ are in accordance with 2 unpaired electrons, as expected for octahedral nickel(II) complexes.

3.1. Crystallographic structures

Single crystals of $[\text{Co}(\text{L}^1\text{H})(\text{L})]$, $[\text{Ni}(\text{L}^1\text{H}_2)_2]\text{Cl}_2$ and $[\text{Ni}(\text{L}^2\text{H}_2)_2]\text{Cl}_2$ suitable for X-ray diffraction studies were grown by slow evaporation of the methanolic solution of these complexes. Mercury rendered ortep projections of $[\text{Co}(\text{L}^1\text{H})(\text{L}^1)]$ and $[\text{Ni}(\text{L}^1\text{H}_2)_2]^{2+}$ showing 50% displacement ellipsoids are given in Fig.1, while that of $[\text{Ni}(\text{L}^2\text{H}_2)_2]\text{Cl}_2$ in SI-F1.

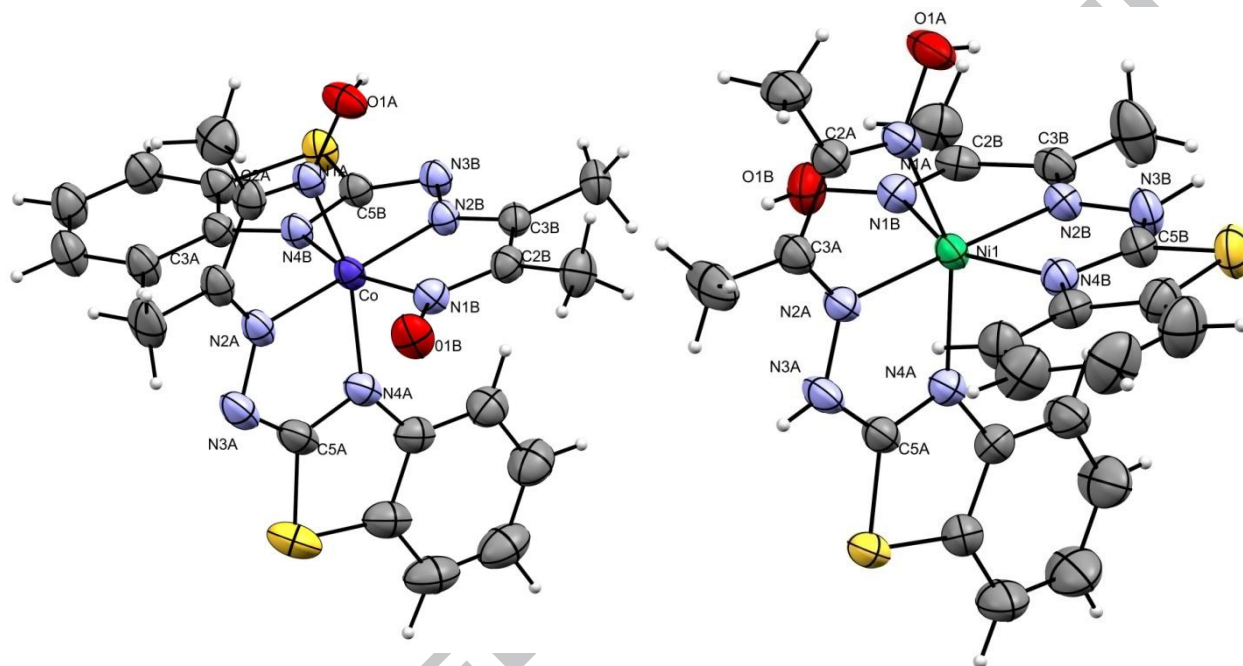


Fig.1. Ortep projections of $[\text{Co}(\text{L}^1\text{H})(\text{L}^1)]$ and $[\text{Ni}(\text{L}^1\text{H}_2)_2]\text{Cl}_2$ showing 50% displacement ellipsoids (Counter anions and crystallization solvents are omitted for clarity).

$[\text{Co}(\text{L}^1\text{H})(\text{L})]$ has crystallized in the monoclinic crystal system with $P2_1/c$ space group while $[\text{Ni}(\text{L}^1\text{H}_2)_2]\text{Cl}_2$ in $P-1$. The asymmetric unit of $[\text{Co}(\text{L}^1\text{H})(\text{L})]$ contains a neutral molecule of the complex without any counter anions. But the asymmetric unit of $[\text{Ni}(\text{L}^1\text{H}_2)_2]\text{Cl}_2$ has $[\text{Ni}(\text{L}^1\text{H}_2)_2]^{2+}$ cation, 2 chloride counter ions along with 3 water molecules. The metal ion is coordinated to two tridentate N, N, N chelators (termed as ligand A and ligand B) in both complexes. Both the ligands have maintained s-cis configuration at the diacetyl fragment. Ligand L^2H_2 , which had s-trans configuration [19] has changed its configuration due to the free rotation of C2-C3 single bond during complexation. In each coordination sphere, both the ligands are practically planar and are almost perpendicular to each other. The mean planes of the two ligands in cobalt and nickel complexes have maintained a dihedral angle of 85.76° and 89.04° respectively. The ligating atoms of ligands being identical in all the cases, the central metal ion is

coordinated in a core of 6 nitrogens. Two tridentate ligands have coordinated in meridional fashion with the ring-N (N4), imine-N (N2) and oxime-N (N1) as donor atoms.

In each complex, azomethine nitrogens of the two ligands (N2A-N2B) reside *trans* to each other whereas the other two donor sites (N1A-N1B and N4A-N4B) have remained mutually *cis* to each other. Though the ligating pattern is same in these complexes, the mutual orientation of two ligands in a complex is found to be different for $[\text{Co}(\text{L}^1\text{H})(\text{L})]$ and $[\text{Ni}(\text{L}^1\text{H}_2)_2]\text{Cl}_2$. This is schematically represented in Fig.2. If this kind of difference in mutual orientation of unsymmetrical tridentate ligands is observed within the two complexes of the same metal ion, that would eventually lead to stereoisomerism [29]. Further, the two nickel complexes, $[\text{Ni}(\text{L}^1\text{H}_2)_2]\text{Cl}_2$ and $[\text{Ni}(\text{L}^2\text{H}_2)_2]\text{Cl}_2$ have shown similar structural features and same spatial orientation of ligands.

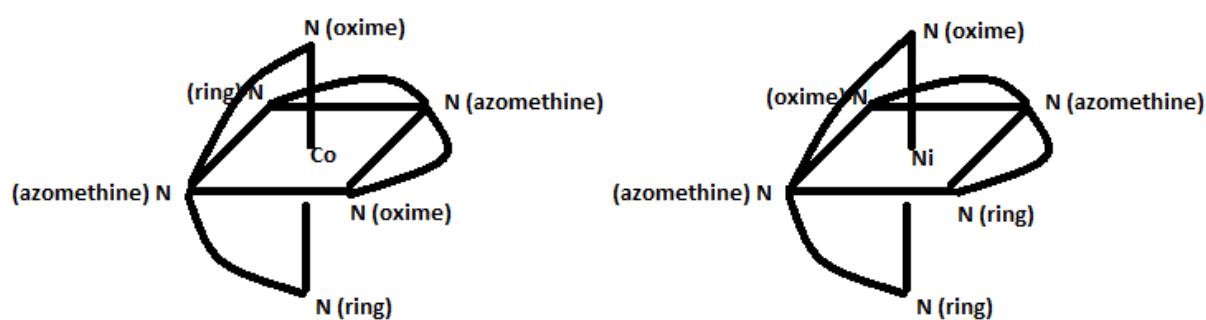


Fig.2. Schematic representation of the mutual orientation of ligands in $[\text{Co}(\text{L}^1\text{H})(\text{L})]$ and $[\text{Ni}(\text{L}^1\text{H}_2)_2]\text{Cl}_2$.

Ligands have formed two five-membered chelate rings with the metal center. The N-M-N bite angles in all the cases have significantly deviated from ideal octahedral bite angle of 90° , indicating significant deviations from ideal octahedral geometry in the complexes.

3.2. Mode of deprotonation through bond length analysis

The ligands used in this investigation has essentially two ionizable protons viz hydrazide-NH and hydroxyl-OH. Hence the ligands can provide N, N, N ligation either in the neutral form or in the anionic form. If the ligand is behaving anionic, it can do so by the deprotonation of either of the 2 ionizable hydrogens or by both. This opens up 4

different modes of deprotonation for the ligand to give the same mode of ligation. These modes are depicted in the Fig.3 for the complexes of benzothiazole based ligand.

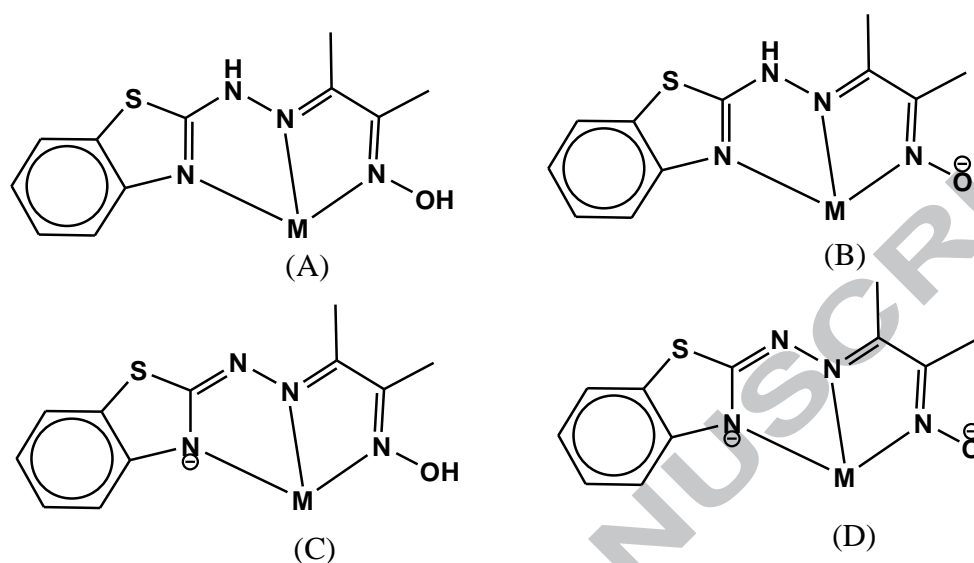


Fig.3. Different modes of deprotonation for the complexes benzothiazole based ligand.

It is very difficult to assign the correct mode of deprotonation of the ligand with spectral techniques. Even in the X-ray structure, exactly locating all the hydrogen atoms from the difference Fourier map is cumbersome. Hence additionally, bond lengths in the structures of $[\text{Co}(\text{L}^1\text{H})(\text{L})]$ and $[\text{Ni}(\text{L}^1\text{H}_2)_2]^{2+}$ can be compared to establish the correct mode of deprotonation of the ligands. Bond lengths of these two structures are compared in Fig. 4.

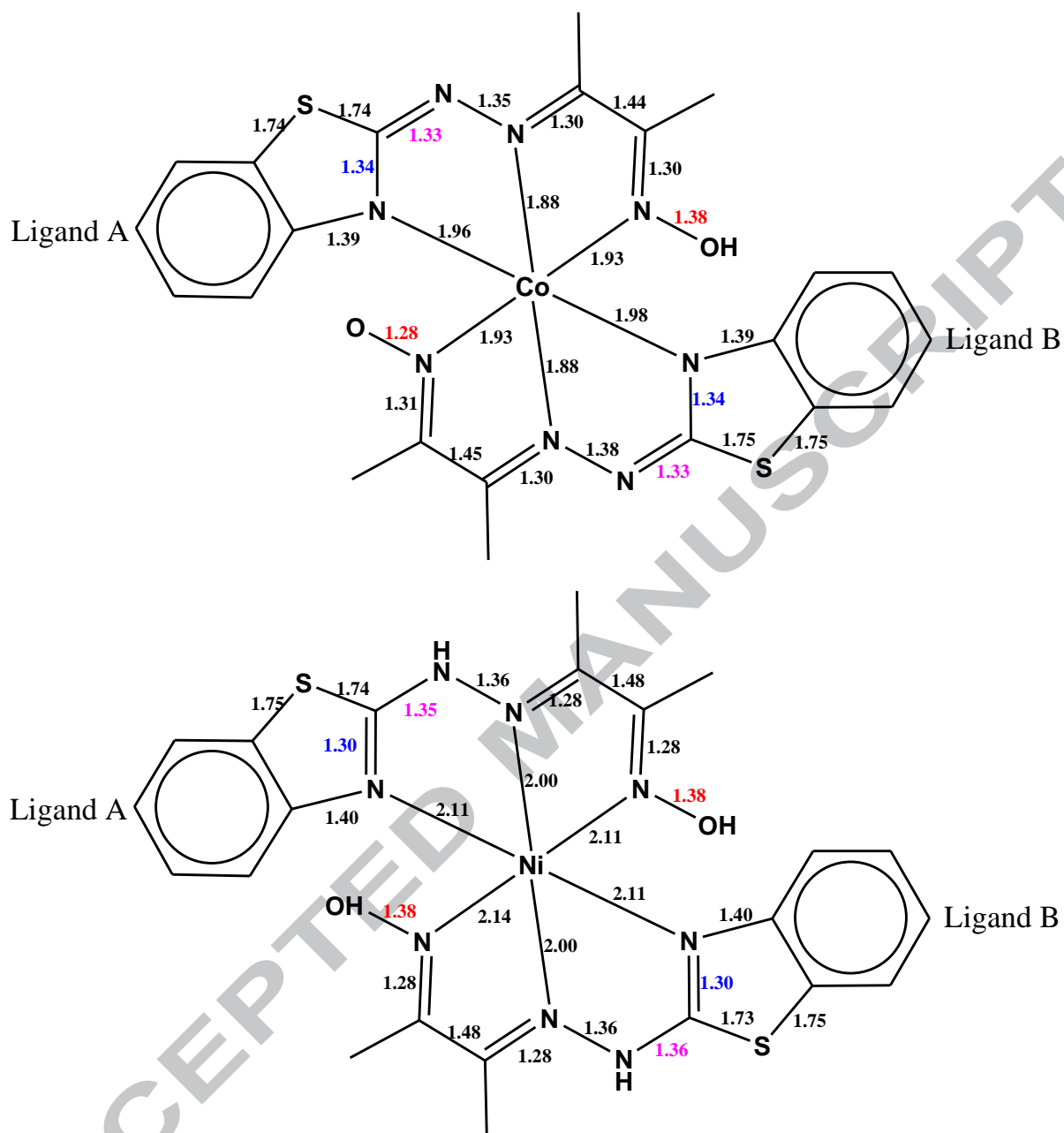


Fig.4. Comparison of bond lengths for [Co(L¹H)(L¹)] and [Ni(L¹H₂)₂]²⁺ (in Å).

In the crystal structure of [Ni(L¹H₂)₂]Cl₂, the presence of two chloride counter anions directly confirms the neutral form (mode A) of both the ligands. But in the structure of [Co(L¹H)(L)], no counter anions are observed suggesting an anionic mode of coordination for both the ligands. Comparison of C5-N4 and C5-N3 bond lengths in the structures, suggest the deprotonation of hydrazide-NH and delocalization of charge, in the ligands of the cobalt complex. In addition, in the ligand B of the cobalt complex, the N1-O1 bond length has reduced to 1.28 Å, indicating a double bond character. This suggests the deprotonation of a hydroxyl group and delocalization of charge acquired on the

oxygen via the conjugated -N=C- groups [30]. Conclusively, in the cobalt complex, the structure of ligand A is close to mode C while the structure of ligand B is close to mode D making the complex heteroleptic. According to the electric neutrality principle, the presence mono-negative and di-negative anions in the cobalt complex eventually confirm the in-situ oxidation of cobalt from 2+ to 3+ oxidation state.

The Co-N bond lengths are in the range of 1.88-1.98 Å while the Ni-N bond lengths are in the order of 2.00-2.11 Å. The shorter bond lengths and stronger coordination which is due to the smaller size of Co(III) ion, is in accordance with the earlier reports for similar Co(III) complexes [12]. Bond length analysis even shows stronger coordination of azomethine nitrogen atoms in both the complexes.

3.3. Mass spectral analysis

The EI mass spectrum of ligands L¹H₂ (SI-F2) and L²H₂ has given molecular ion peaks [M]⁺ at m/z 248 and 231 respectively, corresponding to the exact mass of organic motif. Both the ligands have shown similar fragmentation pattern (SI-F3).

In the positive mode ESI-MS of the cobalt complexes (SI-F4 and SI-F5), base peaks are observed at m/z 553 and 519. This exactly corresponds to the mass of [Co(L¹H)(L¹)+H]⁺ and [Co(L²H)(L²)+H]⁺ species. This assignment is in good agreement with the ascribed +3 oxidation state for cobalt, as cobalt in +2 state would have given these peaks at an m/z of 554 and 520. In the mass spectra (SI-F6 and SI-F7) of nickel complexes, peaks observed at m/z 553 and 519 are assigned to [Ni(L¹H₂)₂-H]⁺ and [Ni(L²H₂)₂-H]⁺ species. The base peaks observed at m/z of 249 and 232 in these complexes are corresponding to [M+H]⁺ species of the of the corresponding ligands.

3.4. Electronic spectral analysis

The free ligand L¹H₂ exhibited broad bands in the UV region at a λ_{max} of 231 and 313 nm respectively. These bands are assigned to the intraligand π→π* and n→π* transitions respectively. L²H₂ has shown these transitions at 218 and 305 nm. These bands have appeared in all the complexes with a slight shift in their λ_{max}. This shift is attributed to the change in π conjugation and coordination of azomethine nitrogens upon complexation [31, 32].

In strong field octahedral cobalt(III) complexes, t_{2g}^6 configuration transforms as $^1A_{1g}$ ground term. Excitation of a electron to e_g level spans $^3T_{1g} + ^3T_{2g} + ^1T_{1g} + ^1T_{2g}$ with low lying spin-triplet states. Hence there are two principal spin-allowed transitions, $^1A_{1g} \rightarrow ^1T_{1g}$ and $^1A_{1g} \rightarrow ^1T_{2g}$ [33, 34]. Cobalt complexes of L^1H_2 and L^2H_2 have shown a new non-ligand band around 487 and 476 nm respectively. The ϵ values and the positions of these peaks fall in the normal range expected for octahedral Co(III) complexes [35, 36]. Due to its high intensity, it may be easily attributed to ligand to Co(III) charge transfer (LMCT) [32, 37]. Further, octahedral Co(III) complexes are expected to show a weak low energy $^1A_{1g} \rightarrow ^1T_{2g}$ transition [38]. In the present case, these transitions are obscured by the broad and intense charge transfer bands [39]. Nickel complexes have shown a very broad band centered at 828 and 818 nm respectively for $[Ni(L^1H_2)_2]Cl_2$ and $[Ni(L^2H_2)_2]Cl_2$. This is assignable to $^3A_{2g} \rightarrow ^3T_{2g}$ transition for an octahedral Ni(II) complex derived from diimine type ligands [40].

3.5. NCI-60 Human Cancer Cell Line Screening

The NCI-60 Human Tumour Cell Lines Screen utilizes 60 different human tumor cell lines, representing leukemia, melanoma and cancers of the lung, colon, brain, ovary, breast, prostate, and kidney cancers to identify and characterize novel compounds with growth inhibition or killing of tumor cell lines. Among all the complexes, the structure of $[Ni(L^1H_2)_2]Cl_2$ was selected by NCI for one dose screening based on its ability to add diversity to the NCI small molecule compound collection.

Growth inhibition percent in single dose assay (10^{-5} M) of $[Ni(L^1H_2)_2]Cl_2$ against 60 human cancer cell lines is summarized in SI-T6. Among the 60 human cancer cell lines tested, the nickel complex derived from benzothiazole core has very effectively inhibited the growth of Non-Small Cell Lung Cancer cell line EKVX (GI %: 73.34) and Breast Cancer cell line MDA-MB-468 (GI %: 69.95). In addition, the compound has even shown considerable activity against Leukaemia cell lines MOLT-4 (GI %: 64.78) and SR (GI %: 65.20). Remaining tested cell lines have shown moderate to less sensitivity towards the compound.

Further to obtain the IC_{50} value of $[Ni(L^1H_2)_2]Cl_2$ against the lung cancer cell line, different concentrations of the drug (300, 150, 75, 37.5, 18.75, 9.375 $\mu g/mL$) of samples

was treated. The obtained cell viability (in%) are 56.94, 61.80, 68.18, 71.79, 75.50 and 83.04 respectively (Negative control : 100%). These results are plotted in Fig.5. The results suggest that the compound exhibit good cytotoxic activities in a concentration dependent manner. The IC_{50} value obtained from the graph is found to be 207.7 $\mu\text{g/ml}$.

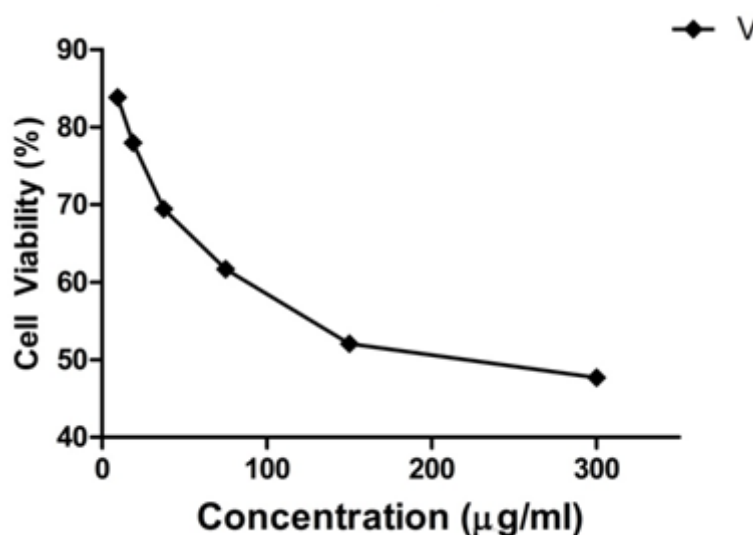


Fig.5. Cytotoxicity of $[\text{Ni}(\text{L}^1\text{H}_2)_2]\text{Cl}_2$ against lung cancer cell line.

3.6. Antibacterial and antifungal assay

Benzothiazole and benzimidazole derivatives are well known antimicrobial agents with chemotherapeutic importance [41]. The antimicrobial potency of newly synthesized ligands and complexes were evaluated against gram-positive bacteria (*S. epidermidis*, *E. faecalis*), gram-negative bacteria (*K. pneumoniae*, *E. coli*) and fungi (*A. fumigatus* and *C. albicans*). Ciprofloxacin and fluconazole were used as standards for antibacterial and antifungal assays respectively. The results are tabulated in table 2.

Table 2. In vitro antimicrobial activity (MIC in $\mu\text{g/mL}$)

Microbial Strains	Gram-positive bacteria		Gram-negative bacteria		Fungi	
	<i>S. epidermidis</i>	<i>E. faecalis</i>	<i>K. pneumoniae</i>	<i>E. coli</i>	<i>A. fumigatus</i>	<i>C. albicans</i>
L^1H_2	0.4	50	3.12	50	0.4	0.4

$L^2H_{2[19]}$	0.8	12.5	0.4	3.12	0.4	0.4
$[Co(L^1H)(L^1)]$	0.8	3.12	0.4	12.5	0.4	0.8
$[Co(L^2H)(L^2)]$	0.4	12.5	0.8	6.25	0.4	0.4
$[Ni(L^1H_2)_2]Cl_2$	0.4	50	6.25	12.5	0.4	0.4
$[Ni(L^2H_2)_2]Cl_2$	1.6	3.12	0.4	12.5	0.8	0.4
Ciprofloxacin	1.6	1.6	0.8	1.6	-	-
Flucanazole	-	-	-	-	16	8

Between the two gram positive bacterial strains, synthesized compounds have shown excellent growth inhibition activity against *S. epidermidis*. Hence the cobalt complexes are 2-4 times more active than the standard, ciprofloxacin. *K. pneumoniae* is found to be sensitive in gram-negative strains. Upon complexation, cobalt complex of L^1H_2 has shown 2-16 fold activity enhancement against gram-negative strains.

According to Overtone's concept of cell permeability, the lipid membrane of the cell favours the passage of lipid-soluble materials. Hence lipophilicity plays an important role in antimicrobial activity. In the case of chelation of a bulky ligand to a metal cation, due to the overlap of the ligand orbitals and partial sharing of positive charge of the metal ion with donor groups, the polarity of the metal ion is significantly reduced[42]. Due to the increased delocalization of the π -electrons over the whole chelate ring, lipophilicity of the complex increases. This enhances the penetration of the complexes into the lipid membrane, which in turn blocks the metal binding sites on enzymes of microorganisms[43]. Hence the metal complexes seem to block the synthesis of proteins and disturb the process of respiration of the cell restricting the further growth. Hence the enhanced activity of cobalt complexes in comparison with nickel complexes could be related to reduced overall polarity of the molecule, which increases the lipophilic nature of the complex, favoring the efficient permeation through lipid layer of the microorganism[44].

Compounds are inhibiting the growth of *A. fumigatus* and *C. albicans* even at a very low concentration of 0.4 $\mu\text{g/mL}$. This makes the complexes very effective against fungal strains, over the tested standard-fluconazole.

4. Conclusions

In the present work two new Schiff base ligands, 3-(hydroxyimino)-2-butanone-2-(1*H*-benzothiazol-2-yl)hydrazone and 3-(hydroxyimino)-2-butanone-2-(1*H*-benzimidazol-2-yl)hydrazone are synthesized and characterized. The ligands bind the metal centers in tridentate mode through ring-N, azomethine-N and oxime-N atoms respectively. Analytical and spectroscopic data for the complexes indicate that the ligands have shown ML₂ type octahedral coordination towards Ni(II) and in situ generated Co(III) ions. [Co(L¹H)(L)] has crystallized in the monoclinic crystal system with *P* 2₁/c space group and [Ni(L¹H₂)₂]Cl₂ in *P* -1. X-ray structures have shown meridional fashion of 2 tridentate ligands to give distorted octahedral geometry to the complexes. From the crystal structures and comparison of bond lengths, it is clear that the ligands have shown the similar mode of ligation, but a different mode of deprotonation with the metal ions. Ligands are left neutral in the case of nickel complexes while anionic in the case of cobalt complexes. Further, *in situ* oxidation of Co(II) to Co(III) has triggered a different mode of deprotonation between the two ligands of the same cobalt complex. Among the 60 human cancer cell lines tested, [Ni(L¹H₂)₂]Cl₂ has very effectively inhibited the growth of Non-Small Cell Lung Cancer cell line EKVX (GI %: 73.34) and Breast Cancer cell line MDA-MB-468 (GI %: 69.95). Further, synthesized compounds have shown excellent growth inhibition activity against *S. epidermidis*. Complexes are even found to be very effective against fungal strains, over the tested standard-fluconazole.

Appendix A. Supplementary data

CCDC 1491779, 1491782 and CCDC 1524740 contains the supplementary crystallographic data for [Co(L¹H)(L)], [Ni(L¹H₂)₂]Cl₂ and [Ni(L²H₂)₂]Cl₂. These data can be obtained free of charge via <http://www.ccdc.cam.ac.uk/conts/retrieving.html>, or from the Cambridge Crystallographic Data Centre, 12 Union Road, Cambridge CB2 1EZ, UK; fax: (+44) 1223-336-033; or e-mail: deposit@ccdc.cam.ac.uk.

Acknowledgements

The authors thank USIC, Karnatak University, Dharwad, for providing spectral and SC-XRD facilities. Recording of ESI-mass spectra from IIT Kanpur and CDRI-Lucknow is greatly acknowledged. NCI-USA is acknowledged for NCI-60 Human

Tumor Cell Lines Screen under Developmental Therapeutics Program. One of the authors (Vinayak Kamat) is thankful to UGC-New Delhi for providing financial assistance under UGC-SRF (101864/June 2013).

References

- [1] J.F. Geldard, F. Lions, Tridentate Chelate Compounds. III, *Inorganic Chemistry*, 2 (1963) 270-282.
- [2] M. Sutradhar, G. Mukherjee, M.G.B. Drew, S. Ghosh, Simple General Method of Generating Non-oxo, Non-amavadine Model Octacoordinated Vanadium(IV) Complexes of Some Tetradentate ONNO Chelating Ligands from Various Oxovanadium(IV/V) Compounds and Structural Characterization of One of Them, *Inorganic Chemistry*, 46 (2007) 5069-5075.
- [3] V.H. Arali, V.K. Revankar, V.B. Mahale, P.J. Kulkarni, Cobalt(II), nickel(II) and copper(II) with 2-substituted benzimidazole complexes, *Transition Metal Chemistry*, 19 (1994) 57-60.
- [4] G.S. Kurdekar, S. Mudigoudar Puttanagouda, N.V. Kulkarni, S. Budagumpi, V.K. Revankar, Synthesis, characterization, antibiogram and DNA binding studies of novel Co(II), Ni(II), Cu(II), and Zn(II) complexes of Schiff base ligands with quinoline core, *Medicinal Chemistry Research*, 20 (2011) 421-429.
- [5] Z.H. Chohan, C.T. Supuran, A. Scozzafava, Metalloantibiotics: Synthesis and Antibacterial Activity of Cobalt(II), Copper(II), Nickel(II) and Zinc(II) Complexes of Kefzol, *Journal of Enzyme Inhibition and Medicinal Chemistry*, 19 (2004) 79-84.
- [6] V. Kamat, D. Kokare, K. Naik, A. Kotian, S. Naveen, S.R. Dixit, N.K. Lokanath, S.D. Joshi, V.K. Revankar, Transition metal complexes of 2-(2-(1H-benzo[d]imidazol-2-yl)hydrazono)propan-1-ol: Synthesis, characterization, crystal structures and anti-tuberculosis assay with docking studies, *Polyhedron*, 127 (2017) 225-237.
- [7] S.E.H. Etaiw, D.M. Abd El-Aziz, E.H. Abd El-Zaher, E.A. Ali, Synthesis, spectral, antimicrobial and antitumor assessment of Schiff base derived from 2-aminobenzothiazole and its transition metal complexes, *Spectrochimica Acta Part A: Molecular and Biomolecular Spectroscopy*, 79 (2011) 1331-1337.
- [8] S.A. Galal, K.H. Hegab, A.M. Hashem, N.S. Youssef, Synthesis and antitumor activity of novel benzimidazole-5-carboxylic acid derivatives and their transition metal complexes as topoisomerase II inhibitors, *European Journal of Medicinal Chemistry*, 45 (2010) 5685-5691.
- [9] J.P. Naskar, C. Biswas, L. Lu, M. Zhu, Synthesis, Crystal Structure and Spectroscopic Properties of an Oximate Bridged Cu(II) Dimer, *Journal of Chemical Crystallography*, 41 (2011) 502-507.
- [10] B. Biswas, S. Salunke-Gawali, T. Weyhermüller, V. Bachler, E. Bill, P. Chaudhuri, Metal-Complexes As Ligands to Generate Asymmetric Homo- and Heterodinuclear MAIIIMBII Species: a Magneto-Structural and Spectroscopic Comparison of Imidazole-N versus Pyridine-N, *Inorganic Chemistry*, 49 (2010) 626-641.
- [11] A. Chakravorty, Structural chemistry of transition metal complexes of oximes, *Coordination Chemistry Reviews*, 13 (1974) 1-46.
- [12] P. Sambasiva Reddy, K. Hussain Reddy, Transition metal complexes of benzil- α -monoxime (BMO); X-ray structure determination of Co(BMO)₃, *Polyhedron*, 19 (2000) 1687-1692.
- [13] M. Sutradhar, L.M. Carrella, E. Rentschler, A Discrete μ_4 -Oxido Tetranuclear Iron(III) Cluster, *European Journal of Inorganic Chemistry*, 2012 (2012) 4273-4278.
- [14] A. Kufelnicki, S.V. Tomy, Y.S. Moroz, M. Haukka, J. Jaciubek-Rosińska, I.O. Fritsky, Synthesis of cobalt(III) complexes with new oxime-containing Schiff base ligands and metal-ligand coordination in solution, *Polyhedron*, 33 (2012) 410-416.
- [15] N. Mondal, D.K. Dey, S. Mitra*, K.M.A. Malik*, Synthesis and structural characterization of mixed ligand η^1 -2-hydroxyacetophenone complexes of cobalt(III), *Polyhedron*, 19 (2000) 2707-2711.
- [16] N. Saha, N. Mukherjee, Synthesis, characterisation and coordinating properties of a new pyrazole-derived thiosemicarbazone, a potential antiviral agent: Co(III), Ni(II) and Cu(II) complexes of

- neutral and deprotonated 5(3)-methylpyrazole-3(5)-aldehydthiosemicarbazone, *Polyhedron*, 3 (1984) 1135-1140.
- [17] R.K. Parashar, R.C. Sharma, A. Kumar, G. Mohan, Stability studies in relation to IR data of some schiff base complexes of transition metals and their biological and pharmacological studies, *Inorganica Chimica Acta*, 151 (1988) 201-208.
- [18] S.M. Annigeri, A.D. Naik, U.B. Gangadharmath, V.K. Revankar, V.B. Mahale, Symmetric binuclear complexes with an 'end-off' compartmental Schiff base ligand, *Transition Metal Chemistry*, 27 (2002) 316-320.
- [19] V. Kamat, K. Naik, V.K. Revankar, Effect of acetate and nitrate anions on the molecular structure of 3-(hydroxyimino)-2-butanone-2-(1H-benzimidazol-2-yl)hydrazone, *Journal of Molecular Structure*, 1133 (2017) 546-556.
- [20] S.P. Bruker, Bruker AXS Inc., Madison, Wisconsin, USA., DOI.
- [21] O.V. Dolomanov, L.J. Bourhis, R.J. Gildea, J.A.K. Howard, H. Puschmann, OLEX2: a complete structure solution, refinement and analysis program, *Journal of Applied Crystallography*, 42 (2009) 339-341.
- [22] G. Sheldrick, SHELXT - Integrated space-group and crystal-structure determination, *Acta Crystallographica Section A*, 71 (2015) 3-8.
- [23] G. Sheldrick, Crystal structure refinement with SHELXL, *Acta Crystallographica Section C*, 71 (2015) 3-8.
- [24] C.F. Macrae, I.J. Bruno, J.A. Chisholm, P.R. Edgington, P. McCabe, E. Pidcock, L. Rodriguez-Monge, R. Taylor, J. van de Streek, P.A. Wood, Mercury CSD 2.0 - new features for the visualization and investigation of crystal structures, *Journal of Applied Crystallography*, 41 (2008) 466-470.
- [25] R.H. Shoemaker, The NCI60 human tumour cell line anticancer drug screen, *Nat Rev Cancer*, 6 (2006) 813-823.
- [26] P. Skehan, R. Storeng, D. Scudiero, A. Monks, J. McMahon, D. Vistica, J.T. Warren, H. Bokesch, S. Kenney, M.R. Boyd, New Colorimetric Cytotoxicity Assay for Anticancer-Drug Screening, *JNCI: Journal of the National Cancer Institute*, 82 (1990) 1107-1112.
- [27] M.R. Boyd, The NCI In Vitro Anticancer Drug Discovery Screen, in: B.A. Teicher (Ed.) *Anticancer Drug Development Guide*, Humana Press Inc., Totowa, NJ, 1997, pp. 23-42.
- [28] M.a.G. Schwabe, Antimicrobial susceptibility testing protocols, CRC Press, DOI (2007).
- [29] A. Mohamadou, K. Ple, A. Haudrechy, Drawing Mononuclear Octahedral Coordination Compounds Containing Tridentate Chelating Ligands, *Journal of Chemical Education*, 88 (2011) 302-305.
- [30] M. Sutradhar, T. Roy Barman, J. Klanke, M.G.B. Drew, E. Rentschler, A novel Cu(II) dimer containing oxime-hydrazone Schiff base ligands with an unusual mode of coordination: Study of magnetic, autoreduction and solution properties, *Polyhedron*, 53 (2013) 48-55.
- [31] D.G. Kokare, V. Kamat, K. Naik, A. Nevrekar, A. Kotian, V.K. Revankar, Evaluation of DNA cleavage, antimicrobial and anti-tubercular activities of potentially active transition metal complexes derived from 2,6-di(benzofuran-2-carbohydrazono)-4-methylphenol, *Journal of Molecular Structure*, DOI <http://dx.doi.org/10.1016/j.molstruc.2016.07.072>.
- [32] D. Bandyopadhyay, M. Layek, M. Fleck, R. Saha, C. Rizzoli, Synthesis, crystal structure and antibacterial activity of azido complexes of cobalt(III) containing heteroaromatic Schiff bases, *Inorganica Chimica Acta*, 461 (2017) 174-182.
- [33] S.M. Soliman, J.H. Albering, M. Farooq, M.A.M. Wadaan, A. El-Faham, Synthesis, structural and biological studies of two new Co(III) complexes with tridentate hydrazone ligand derived from the antihypertensive drug hydralazine, *Inorganica Chimica Acta*, 466 (2017) 16-29.
- [34] S. Chattopadhyay, M.G.B. Drew, A. Ghosh, Methylene Spacer-Regulated Structural Variation in Cobalt(II/III) Complexes with Bridging Acetate and Salen- or Salpn-Type Schiff-Base Ligands, *European Journal of Inorganic Chemistry*, 2008 (2008) 1693-1701.

- [35] S. Anjana, S. Donring, P. Sanjib, B. Varghese, N.N. Murthy, Controlling the oxidation of bis-tridentate cobalt(II) complexes having bis(2-pyridylalkyl)amines: ligand vs. metal oxidation, Dalton Transactions, DOI 10.1039/C7DT01792H(2017).
- [36] W.A. Hoffert, M.K. Kabir, E.A. Hill, S.M. Mueller, M.P. Shores, Stepwise acetylide ligand substitution for the assembly of ethynylbenzene-linked Co(III) complexes, *Inorganica Chimica Acta*, 380 (2012) 174-180.
- [37] K. Ghosh, K. Harms, S. Chattopadhyay, Synthesis, characterization and phenoxazinone synthase mimicking activity of cobalt(III) Schiff base complexes, *Polyhedron*, 123 (2017) 162-175.
- [38] L. Pogány, J. Moncol, M. Gál, I. Šalitroš, R. Boča, Four cobalt(III) Schiff base complexes – Structural, spectroscopic and electrochemical studies, *Inorganica Chimica Acta*, 462 (2017) 23-29.
- [39] L.A. Berben, J.R. Long, Homoleptic Trimethylsilylacetylide Complexes of Chromium(III), Iron(II), and Cobalt(III): Syntheses, Structures, and Ligand Field Parameters, *Inorganic Chemistry*, 44 (2005) 8459-8468.
- [40] M.A. Robinson, J.D. Curry, D.H. Busch, Complexes Derived from Strong Field Ligands. XVII. Electronic Spectra of Octahedral Nickel(II) Complexes with Ligands of the α -Diimine and Closely Related Classes, *Inorganic Chemistry*, 2 (1963) 1178-1181.
- [41] İ. Yalçın, İ. Ören, E. Şener, A. Akin, N. Uçartürk, The synthesis and the structure-activity relationships of some substituted benzoxazoles, oxazolo(4,5-b)pyridines, benzothiazoles and benzimidazoles as antimicrobial agents, *European Journal of Medicinal Chemistry*, 27 (1992) 401-406.
- [42] P. Jigna, I. Pranav, N. Rathish, B. Shipra, C. Sumitra, Synthesis and antibacterial activity of some Schiff bases derived from 4-aminobenzoic acid, *Journal of the Serbian Chemical Society*, 70 (2005) 1155-1162.
- [43] V.Y. Kumar, N. Rathish, S. Mayur, B. Shipra, S. Sumitra, Synthesis, structural determination and antibacterial activity of compounds derived from vanillin and 4-aminoantipyrine, *Journal of the Serbian Chemical Society*, 69 (2004) 991-998.
- [44] D.G. Kokare, K. Naik, A. Nevrekar, A. Kotian, V. Kamat, V.K. Revankar, Synthesis and spectroscopic characterization of transition metal complexes derived from novel benzofuran hydrazone chelating ligand: DNA cleavage studies and antimicrobial activity with special emphasis on antituberculosis, *Applied Organometallic Chemistry*, DOI 10.1002/aoc.3413(2016) n/a-n/a.

Graphical abstract

